Clean Technologies and Environmental Policy
https://doi.org/10.1007/s10098-024-02844-9

ORIGINAL PAPER

Low-hazardous multi-functional textile through one-step nano-assisted processing

Seyed Mohammad Taher Shahin[1] · Majid Montazer[2] · Mahnaz Mahmoudirad[3]

Received: 2 December 2023 / Accepted: 30 March 2024

Abstract

Textile processing with low hazardous chemicals in one step through a nano-assisted technique for multi-functional purposes is an important task. Here, the toxic carrier was replaced with zinc acetate in dyeing to modify the polyester fabric through the synthesis of zinc oxide nanoparticles (ZnO-NPs), whereas polyester after conventional dyeing was followed by other required finishing to achieve functional properties. Disperse blue 19 and zinc acetate were used on different pre-treated fabrics at 130 °C for 1 h in diverse alkaline media. The dyeing effluent showed almost no remaining dye providing a clean route for the simultaneous nano-assisted processing. This eco-friendly, time-, and energy-saving technique exhibited an even distribution of ZnO-NPs on the fabric with reasonable dye adsorption. NaOH, as an alkaline, caused the smallest ZnO-NPs with the highest evenness. However, applying air plasma as a clean activation route on the fabric alongside alkali processing produced a higher color strength with the lowest cytotoxicity. Furthermore, the mechanical, physical, and chemical properties of polyester fabrics improved as noticeable achievements. Besides, excellent color fastness against washing, rubbing, and light obtained on all dyed and ZnO-NPs synthesized samples indicated the successful attachment of dye and nanoparticles on the fabric. In addition, the efficient product showed antibacterial features against *S. aureus*. Lastly, better stability in alkaline media specified for the dyed fabric included synthesized ZnO-NPs which led to an industrially advanced multi-functional product.

✉ Majid Montazer
tex5mm@aut.ac.ir

[1] Department of Textile Engineering, Functional Fibrous Structures and Environmental Enhancement (FFSEE), Amirkabir University of Technology, Tehran, Iran

[2] Department of Textile Engineering, Functional Fibrous Structures and Environmental Enhancement (FFSEE), Amirkabir Nanotechnology Research Institute (ANTRI), Amirkabir University of Technology, Tehran, Iran

[3] Skin Research Centre, Shahid Beheshti University of Medical Sciences, Tehran, Iran

Published online: 29 April 2024

Graphical abstract

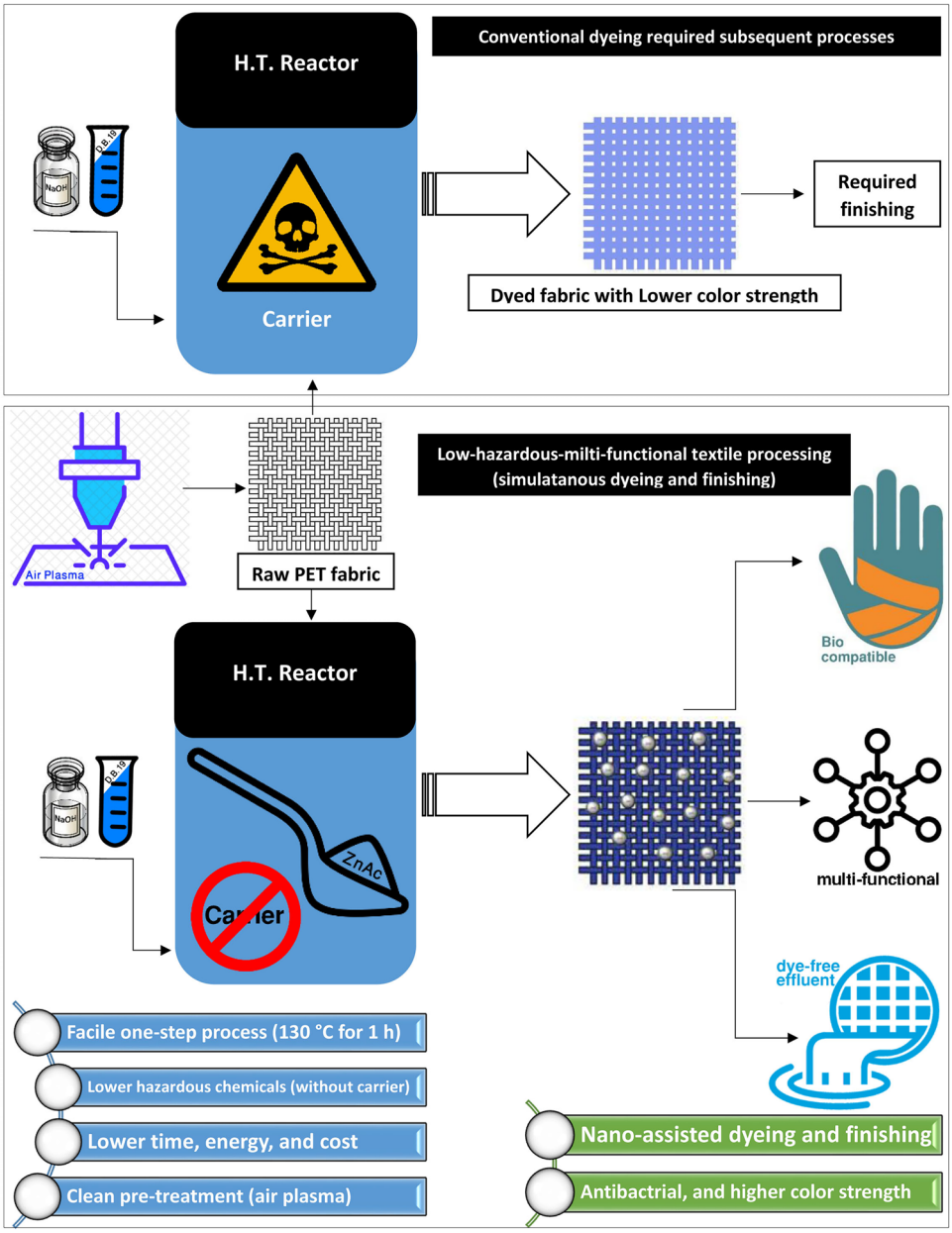

Keywords Antibacterial properties · Dye-free effluent · Eco-friendly · In situ synthesis and dyeing · Multi-functional properties · Polyester fabric · Zinc oxide nanoparticles

Introduction

Disperse dyes are the main category of dyes utilized in the PET fibers dyeing that are used at 130 °C or boiled alongside the carrier, or the PET first impregnated in the dye bath with suitable dispersants, then dried, and cured at 190–220 °C (Nunn 1979). Carrier by improving dye uptake, quickening rate of dyeing, and reducing the heat of dyeing can decrease glass transition temperature (T_g) (Arcoria et al. 1985). Environmental contamination, toxicity, and unpleasant odor are the main problems of most carriers (Choudhury 2006). Therefore dyeing without a carrier requires more attention to be considered; for example, Harifi and Montazer used nano-TiO_2 for

dyeing polyester fabric with disperse dyes without a carrier. Pre-treating PET with nano-TiO_2 affected the dyeing adsorption positively, and more nano-TiO_2 usage produced higher *K*/*S* (color strength). This is free from the disadvantages of dyeing with a carrier, for example, toxicity (Harifi and Montazer 2013).

Besides, other methods of coloration were considered, such as PET dyeing with microencapsulated disperse dyes without dispersing agents, penetrating agents, leveling agents, or other auxiliaries. In this manner, the quality of dyed polyester fabric without reduction clearing was at least as good as traditionally dyed fabric after washing and reduction clearing (Yi et al. 2005). Also, Bhuiyan et al. reported PET dyeing with henna at various temperatures deprived of utilizing dangerous metallic dye fixatives. The dye absorption by fiber and the subsequent shade deepness increased at a higher temperature (Bhuiyan et al. 2018).

Rezaie et al. used eco-friendly joint CuO-NPs to nano-colorize wool fibers in a one-step process as a green and economical method. The process was done with copper acetate solution non-polluting reduction on the wool fabric in alkali media, resulting in antibacterial effects and tensile strength improvement with good color fastness (Rezaie et al. 2017). Also, Ahmed et al. prepared PET fabric with four different disperse dyes in an aqueous solution of polyethylene glycol with 100% pick-up. Polyethylene glycol acted as a fiber plasticizer, and the swelling agent produced excellent color indices, leveling, and fastness properties (Ahmed et al. 2020).

Meanwhile, zinc oxide was used in anti-corrosion, anti-bacterial, and UV absorbent products as relatively bio-safe and biocompatible material. Moreover, it was discovered that nanostructured metal oxide exhibits desirable morphological, functional, biocompatible, non-toxic, and catalytic properties (Hasnidawani et al. 2016; Wahab et al. 2013). Therefore, making these nanoparticles from their acetate salt is thought to be a safe alternative to using dye carriers.

Moreover, the low wettability and lack of polyester (PET) functional groups cause difficulties in dyeing and finishing. Several methods were used to solve these problems, such as hydrolysis, aminolysis, and plasma treatment before dyeing and finishing (Mirjalili and Karimi 2013; Afshari et al. 2019).

There are some reports on the local fabrication of ZnO nanoparticles (ZnO-NPs) on PET fabrics. Aminolysis and in-position production of ZnO-NPs of PET were concurrently accomplished using triethanolamine (TEA) and zinc acetate (Poortavasoly and Montazer 2014). Also, ZnO-NPs are produced with suitable quality through hydrothermal growth using zinc acetate and sodium hydroxide. The sodium hydroxide yielded a higher production than hexamethylenetetramine (HMTA). In addition, no solvent or calcination is required to obtain different morphologies by using NaOH in various concentrations (Osman and Mustafa 2015). Further, zinc oxide nanoparticles and the hydrolysis of polyester fabric were done by sodium hydroxide at different conditions, ultrasound, and stirrer resulting in spherical and rod-shaped ZnO-NPs (Mohammadi et al. 2016).

Air plasma was already used as a green and environmentally friendly activator to enhance the wettability, wicking, and decreasing soiling of polyester fabric (Morent et al. 2008; Yaman et al. 2009; Samanta et al. 2009; Raffaele-Addamo et al. 2003; Singh and Qureshi 2005). For instance, Kerkeni et al. used atmospheric air plasma as a pre-activator on polyester fabric, and better wettability and dyeing were reported with curcumin at 90 and 130 °C (Kerkeni et al. 2012). Also, nanosilver better adhesion was reported on raw polyester pre-treated with Ar/N_2 plasma (Gorenšek et al. 2010). Ebrahimi et al. stated that plasma treatment improved the performance of various ionic lubricants on polyester fabric. The atmospheric air plasma-treated fabric coated with anionic, cationic, and non-ionic emulsions showed more surface reactivity toward different ionic emulsions (Ebrahimi et al. 2011).

It is clear that the conventional dyeing and finishing of PET fabric is multi-step processing, including 3 or 4 different steps of NPs synthesis, dyeing, and fixing, and is regarded as a time-consuming process. Moreover, due to the carrier, it is significantly hazardous without considering its environmental harmfulness. Here, it was hypothesized that zinc acetate with acetate group replaced the carrier possibly attracted by the ester groups of PET fabric, leading to more interaction of amino groups of disperse dye with the polyester chains. In this study, for the first time, the simultaneous disperse dyeing, and in situ production of ZnO-NPs on PET fabric was reported at 130 °C for 1 h. It means that alongside creating a fabric with multi-functional features through more cost-and time-effective methods in a one-step procedure, the carrier-free nano-assisted method led to an eco-friendly product with free-dye effluent. This was done without alkali and with various alkalis, including NaOH and Na_2CO_3. In addition, the influence of air plasma pre-treatment as a clean physical surface activator was investigated. Finally, this clean route eventuated the lowest environmental contamination. FT-IR spectroscopy, UV–Vis spectroscopy, light, washing and rubbing fastness, tensile, crease recovery angle, bending length, and air permeability tests were carried out to confirm the synthesized nanoparticles on the surface and show the shade, depth, and strength of dye without a carrier and other properties of the dyed fabrics. Antibacterial tests and alkali resistance were also

considered offering reasonable bacteria killing and good stability against alkali media. Finally, the various dyeing effluents were considerably reasonable regarding color, as almost no dye molecule can be found in the remaining dye baths.

Experimental

Materials and methods

A 100% polyester fabric with a weight of 88 g/m^2 was provided from Hejab, ShahreKord, Iran and zinc acetate dihydrate ($Zn(CH_3COO)_2{\cdot}2H_2O$, 219.49 g/mol, NaOH, and Na_2CO_3 were purchased from Merck Co. Germany. C.I. Disperse Blue 19 was provided by ex-Ciba (Swiss) with the structure presented in Fig. 1.

The plasma instrument was used from Adecco Co, Iran, with a speed of 5 m/min, power of 2.7 KW, and passage of 12 rounds.

Initially, washing of fabric was done in a bath containing 1 g/L non-ionic detergent with L:G = 50:1 (liquor to good ratio) at 60 °C for 20 min before synthesis and dyeing. Next, it was washed with purified water and dehydrated at ambient conditions.

HT reactor was used in all experiments of in situ fabrication of ZnO-NPs. The settings and materials used are shown in Table 1. In this table the following abbreviations were used: R = raw material + dye, Zn = raw material + zinc acetate + dye, ZnP = raw material + zinc acetate + dye + air plasma pre-treatment, Hy = raw material + dye + sodium hydroxide, HyZn = raw material + zinc acetate + dye + sodium hydroxide, HyZnP = raw material + zinc acetate + dye + air plasma pre-treatment + sodium hydroxide, C = raw material + dye + sodium carbonate, CZn = raw material + zinc acetate + dye + sodium carbonate, CZnP = raw material + zinc acetate + dye + air plasma pre-treatment + sodium carbonate. The synthesis was performed in HT reactor at 130 °C with L:G = 150:1 for 1 h.

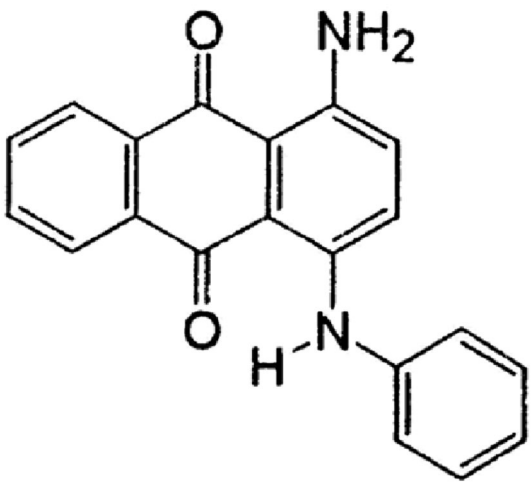

Fig. 1 Chemical structure of C.I. Disperse Blue 19

Characterization

The synthesized ZnO-NPs on the polyester fabric were distinguished with Fourier transform infrared (FT-IR) spectroscopy with Nicolet spectrometer (France) to investigate the surface chemical changes and synthesis of ZnO-NPs PET fabrics.

X-ray diffraction analysis (XRD) (Siemens D5000) was used to determine the presence and type of deposited nanoparticles on the surface of polyester fabric with CuKα radiation source ($\lambda = 1.541874$°A) at 40 kV.

A color eye XTH spectrophotometer (standard illuminant D65/10°) was employed for assessing the shade of dyed fabrics, which three color coordinates including L^* (lightness), a^* (redness-greenness), and b^* (yellowness-blueness) were used. ΔE of dyed fabrics was calculated by Eq. (1), and it is the difference between the dyed sample compared with the untreated one (Andreola et al. 2008).

$$\Delta E = [(L_2^* - L_1^*)^2 + (a_2^* - a_1^*)^2 + (b_2^* - b_1^*)^2]^{0.5} \quad (1)$$

Table 1 Experimental conditions for preparing various polyester fabric samples in high temperature (HT) for 1 h

Experiments	1			2			3		
Samples	R[a]	Zn[a]	ZnP[a]	Hy[a]	HyZn[a]	HyZnP[a]	C[a]	CZn[a]	CZnP[a]
Zinc acetate (owf %)	–	10	10	–	10	10	–	10	10
Dye (1% owf)	+	+	+	+	+	+	+	+	+
Air plasma Pre-treatment	–	–	+	–	–	+	–	–	+
NaOH (pH = 10)	–	–	–	+	+	+	–	–	–
Na_2CO_3 (pH = 10)	–	–	–	–	–	–	+	+	+

[a]*R* raw material, *Zn* zinc acetate, *P* air plasma pre-treatment, *Hy* sodium hydroxide, *C* sodium carbonate

From Eq. (2), the weight variation percentage ($\Delta W\%$) of the dyed and synthesized fabrics was evaluated, with determining weights of the samples before (W_1) and after (W_2) the curing:

$$\Delta W\% = \left[\left(W_2 - W_1\right)/W_1\right] \times 100 \quad (2)$$

An Instron (USA) was used to study the tensile strength of treated and untreated fabrics. A 10-cm gauge distance, a broadening amount of 75 mm/min, and a 10,000-N load cell were used. Samples were cut to 15×3 cm^2 tested three times, and the average was reported. The stiffness tester of Shirley was utilized for analyzing the bending length of the fabrics in the warp direction. Another Shirley instrument was utilized to determine the crease recovery angle of cut samples to 1×2 inch^2. The treated fabrics were folded in the warp direction and located below the weight of 1 kg for 1 min. After the pressure was removed, the treated fabrics were rested for 1 min. Finally, the angle among the two exposed ends of the treated fabric was verified. Three repeats were executed for all the mechanical properties tests, and the mean and variation coefficient (CV %) were stated.

The air permeability of treated and raw samples also was calculated by the Shirley device, each one 5 times, and the average of the results and CV % was stated.

The antibacterial property of nano-zinc oxide dyed polyester samples was investigated derived from the measurable test procedure (AATCC-100) concerning both *Staphylococcus aureus* as a Gram-positive and *Escherichia coli* as a Gram-negative pathogenic bacteria. The reduction of bacteria in treated samples was specified in Eq. (3):

$$R\% = \left[(A - B)/A\right] \times 100 \quad (3)$$

where R, A, and B are the percentage of bacteria reduction, and the number of bacterial colonies from control and treated samples, respectively.

The cytotoxicity of dyed PET/ZnO-NPs samples was analyzed via standard main human skin fibroblast dependent on ISO 10993-5 (biological evaluation of medical devices-part 5-tests for vitro cytotoxicity) (ISO 1999). The cell viability percentage was studied by assessing the solution's absorbance of cured (abs_{sample}) and raw ($abs_{control}$) samples using Eq. (4):

$$\text{Cell viability}\,(\%) = \left(abs_{sample}/abs_{control}\right) \times 100 \quad (4)$$

Here the standard main human skin fibroblast was utilized for the cytotoxicity investigation. Fibroblasts were cultured in DMEM (1X) + GlutMAX™ added with 10% fetal calf serum (FCS), protected in a moistened ambient at 37 °C and 5% CO_2. Cells were transferred to a 21-well plate and protected for 24 h. Pristine PET and treated samples were cut into 1×1 in^2 and soaked in 2 ml nutrient agar for 24 h. The nutrient agar with leakage ingredients was supplemented to the cultured cells and protected for 24 h. The cells were reincubated for an additional 24 h in a new medium and afterward verified with 3-(4,5-dimethylthiazol-2-yl)-2,5-diphenyltetrazolium bromide (MTT) examination. The absorbance of each sample (including raw and control) was calculated three times at 570 nm.

The color fastness properties to light, wash, and rub for treated samples were examined according to ISO 105-B01, ISO 105-C10, and ISO 105-X12 standard methods (Chrysler 1990; Yılmaz 2020).

The produced ZnO-NPs on the polyester fabric were characterized with field emission scanning electron microscopy (FESEM) via MIRA3 TESCAN-XMU, the Czech Republic, provided energy-dispersive spectroscopy (EDS) to distinguish the component structure. The FESEM power variety was between 3 and 30 kV, and the images were taken at a power of 15 kV. Particle sizes, shapes (morphologies), and distribution of nanoparticles were determined by image analysis of FESEM pictures.

Alkali resistance was also done on samples using a 50 mL boiling solution of 20% (w/v) sodium hydroxide in 55 min. In addition, the solution color, time of degradation, and shape of decomposed samples were reported.

The various dyeing effluents were recognized with UV–Vis spectroscopy to study the amount of remaining dye in the effluents.

Results and discussion

Synthesis of ZnO-NPs with dyeing in non-alkali media

The polyester fabric was treated with the synthesis of ZnO-NPs alongside dyeing in the H.T. reactors at 130 °C. After 1 h, the blue-dyed samples with different shades were removed from the reactors and washed and tested.

The mechanisms of chemical reactions between zinc acetate (as the precursor) and PET fabric are described in reactions 5–12:

$$Zn\left(CH_3COO\right)_2 + H_2O \rightarrow Zn^{2+} + 2CH_3COO^- \quad (5)$$

$$H_2O \rightarrow OH^- + H^+ \quad (6)$$

$$H^+ + CH_3COO^- \rightarrow CH_3COOH \quad (7)$$

$$Zn^{2+} + 2OH^- \rightarrow Zn(OH)_2 \quad (8)$$

$$Zn(OH)_2 \xrightarrow{\text{Dehydration}} ZnO + H_2O \quad (9)$$

$$nZn(OH)_2 \rightarrow (ZnO)_n + nH_2O \quad (10)$$

$$PET - COO - PET + Zn(OH)_2 \rightarrow PET - OH + PET - COO - Zn(OH) \quad (11)$$

$$PET - COO - Zn(OH) + nZn(OH)_2 \rightarrow PET - COO - (ZnO)_n + nH_2O \quad (12)$$

In reaction 5, hydrolysis of zinc acetate, and in reactions 8–10, two nucleation and growth steps of ZnO nanoparticles are considered. The $Zn(OH)_2$ as Zn nuclei in the first step was formed and then changed to ZnO and H_2O because of dehydration. After that, more ZnO in the media proceeded to the creation of nZnO-NPs (Growth). The modified PET reacts with Zn nuclei ($Zn(OH)_2$) (reaction 11) to form Zn(OH), followed by the growth of ZnO-NPs (reaction 12). The air plasma pre-treatment, dyeing, and in situ synthesis of ZnO-NPs is displayed in Fig. 2. It seems that treating the PET surface with plasma leads to the formation of OH and COO radicals on the surface causes possible reactions with Zn^{2+} ions from one side, and the amine (NH_2) group of the dye from the other side forms organo-metallic complexes. Besides, these ions can make bigger complexes among two amine groups of two dye molecules resulting in a stronger linkage between dye molecules and the fabric surface alongside physical entrapments.

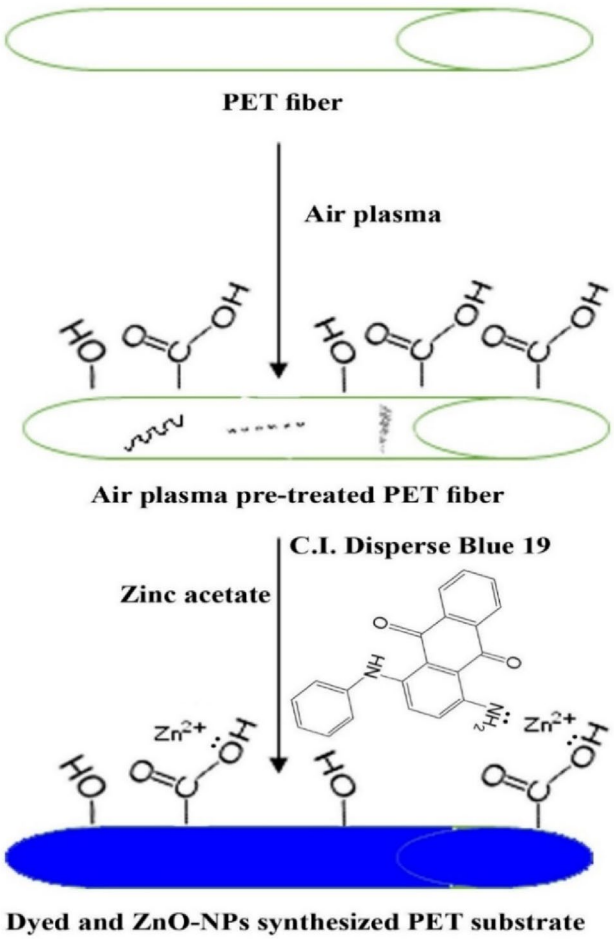

Fig. 2 Schematic of physically activated PET by air plasma, dyeing with disperse dye along with in situ synthesis of ZnO-NPs

Synthesis of ZnO-NPs with dyeing in alkali media

It has already been proved that alkaline media causes a smaller and better distribution of nanoparticles on substrates (Alias and Mohamad 2014). Here, various alkaline (NaOH and Na_2CO_3) were used in the synthesis process to compare them. The chemical reactions between zinc acetate and sodium hydroxide are described in reactions 13–15 (Oskam 2006; Du et al. 2004; Li et al. 1999; Uekawa et al. 2004):

$$Zn(CH_3COO)_2.2H_2O + 2NaOH \rightarrow Zn(OH)_2 + 2CH_3COONa + 2H_2O \quad (13)$$

$$Zn(OH)_2 + 2H_2O \rightarrow Zn(OH)_4^{2-} + 2H^+ \quad (14)$$

$$Zn(OH)_4^{2-} \rightarrow ZnO + H_2O + 2OH^- \quad (15)$$

The ZnO nanostructure formation mechanism is a complex process that is mostly considered in the two key stages of ZnO nuclei generation and ZnO crystal growth. $Zn(OH)_4^{2-}$ compounds attend as fundamental growing parts for the fabrication of ZnO-NPs. Zinc acetate may first change to $Zn(OH)_2$ colloids in alkali media, as presented in reaction 13, and then part of $Zn(OH)_2$ colloids dissociates to Zn^{2+} and OH^- ($Zn(OH)_4^{2-} + 2H^+$) based on reaction 14.

Finally, ZnO can be grown according to reaction 15 at the supersaturation degree of Zn^{2+} and OH^- concentration. In other words, at pH ≥ 8.0, $Zn(OH)_4^{-2}$ with a dehydration reaction (and since OH^- at balance contains the high chemical potential of), can be converted to ZnO (Uekawa et al. 2004).

The final multifunctional dyed and ZnO-NPs in situ synthesized PET substrate are demonstrated in Fig. 3.

The chemical reactions between zinc acetate and sodium carbonate are described in reactions 16–22:

$$Na_2CO_3 + H_2O \rightarrow 2Na^+ + CO_3^{2-} + H_2O \quad (16)$$

$$CO_3^{2-} + H_2O \rightarrow HCO_3^- + OH^- \quad (17)$$

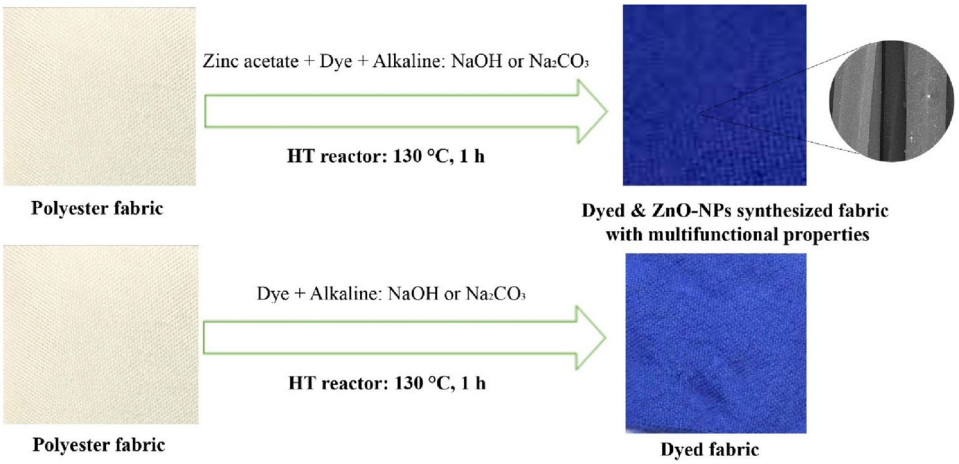

Fig. 3 Schematic of in situ production and loading of ZnO-NPs alongside carrier-free dyeing of PET fabric

$$HCO_3^- + H_2O \rightarrow H_2CO_3 + OH^- \quad (18)$$

$$Zn^{2+} + 2OH^- \rightarrow Zn(OH)_2 \quad (19)$$

$$Zn(OH)_2 + 2OH^- \rightarrow Zn(OH)_4^{2-} \rightarrow ZnO + 2OH^- + H_2O \quad (20)$$

$$Zn\left(CH_3COO\right)_2 + 6OH^- + 3Zn^{2+} \rightarrow 2Zn_2(OH)_3\left(CH_3COO\right) \quad (21)$$

$$Zn_2(OH)_3\left(CH_3COO\right) \rightarrow 2ZnO + CH_3COOH + H_2O \quad (22)$$

The alkaline solution of sodium carbonate supplied the essential hydroxyl ions ($–OH^-$) in the production bath. Then, zinc salt hydrolyzes in the alkaline solution and forms zinc hydroxide, which turns to $Zn(OH)_4^{2-}$ as a metastable complex and produces the essential amount of OH^- ions. This substitute with acetate ion makes $Zn_2(OH)_3(CH_3COO)$ in little OH^- ions extent. Finally, $Zn_2(OH)_3(CH_3COO)$/$Zn(OH)_4^{2-}$ turns to ZnO at high temperatures.

The sodium carbonate as an alkali source attacks the PET structure generating hydroxyl ($–OH^-$) and carboxylate ($–COO^-$) functional groups (Reaction 23):

$$PET - COO - PET + OH^- \rightarrow PET - COO^- + HO - PET \quad (23)$$

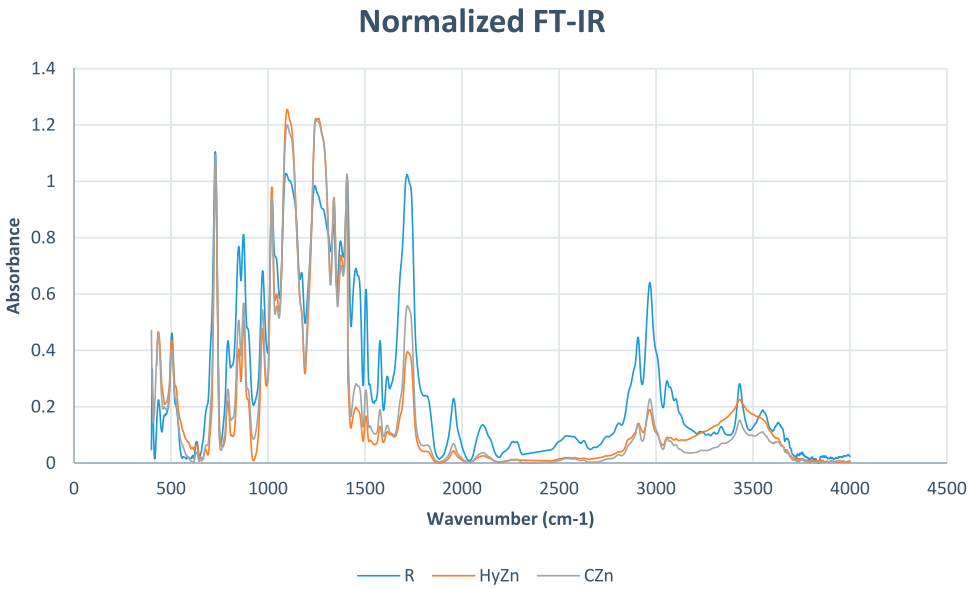

Fig. 4 Normalized FT-IR patterns of various samples

The modified PET performed as an active site for the formation of ZnO-NPs on the polyester (reaction 24):

$$PET - COO^- + Zn^{2+} + 2OH^- \rightarrow PET - COOZnO + H_2O \quad (24)$$

Here dyeing with the synthesis of ZnO-NPs was carried out using 1 owf % dye and other required chemicals such as alkaline and zinc salt. Then warm water was used for rinsing the dyed fabric, and reduction clearing was carried out for 30 min at 60 °C using a 50:1 liquor ratio in a bath containing 10 owf % NaOH and 10 owf % $Na_2S_2O_4$ to eliminate extra dye and auxiliaries.

FT-IR analysis

The FT-IR spectra were normalized at 1410 cm^{-1}. In general, this band (in-plane bending of ring C-H coupled with stretching of ring C–C) is considered insensitive and often used as a reference band to normalize spectral intensity (Dave et al. 2014). Figure 4 clarifies the FT-IR results of R, HyZn, and CZn samples. It is clear that alkali reduced some important peaks, such as 2908 and 2967 cm^{-1} correlated to C–H stretching vibration; 1716 cm^{-1}, sharp peak interrelated to C=O vibration in the ester group, and 1577 and 1614 cm^{-1}corresponded to C–C stretching vibration.

The peaks at 1019, 1099, 1260, and 1339 cm^{-1} are associated with C–O stretching vibration in ester and carboxylic acid; 3431 cm^{-1} corresponds to O–H of hydroxyl group stretching vibration, and 729, 875, and 972 cm^{-1} are associated with C–H bending vibration, C–H (out-of-plane CH=CH bending), and C–H (in-plane CH=CH bending) correspondingly (Afshari et al. 2019; Allahyarzadeh et al. 2013; Küçük and Öveçoğlu 2018). Finally, the nanoparticles cause an immense shift in the FT-IR peak. The peak revealed between 550 and 453 cm^{-1} (504 cm^{-1} in this study) indicated the conversion of $Zn(OH)_2$ to ZnO. The ZnO peak amid 464 and 419 cm^{-1} (434 cm^{-1} in this study) was previously reported (Anna et al. 2008; Li et al. 2004; Ghule et al. 2006). Thus, the peaks at 434 and 504 cm^{-1} can be related to ZnO-NPs that can approve the successful production of ZnO-NPs on the surface of the fabric.

XRD analysis

XRD patterns of five different samples are depicted in Fig. 5. Those peaks at 2Θ = 17–25° are related to the crystalline part of polyester (Harifi and Montazer 2014a; Poortavasoly et al. 2014). The sample R without zinc salt showed no considerable difference; however, a shoulder can be seen at 2Θ = 17°. The synthesized samples, especially HyZn using sodium hydroxide, indicated six different peaks at (100), (002), (101), (102), (110), and (103) planes identified in 2Θ = 31.88, 34.55, and 36.48° confirmed the hexagonal structure of *Wurtzite* according to JCPDS file No. 36-1451. Besides, no other peaks related to $Zn(OH)_2$ can be seen.

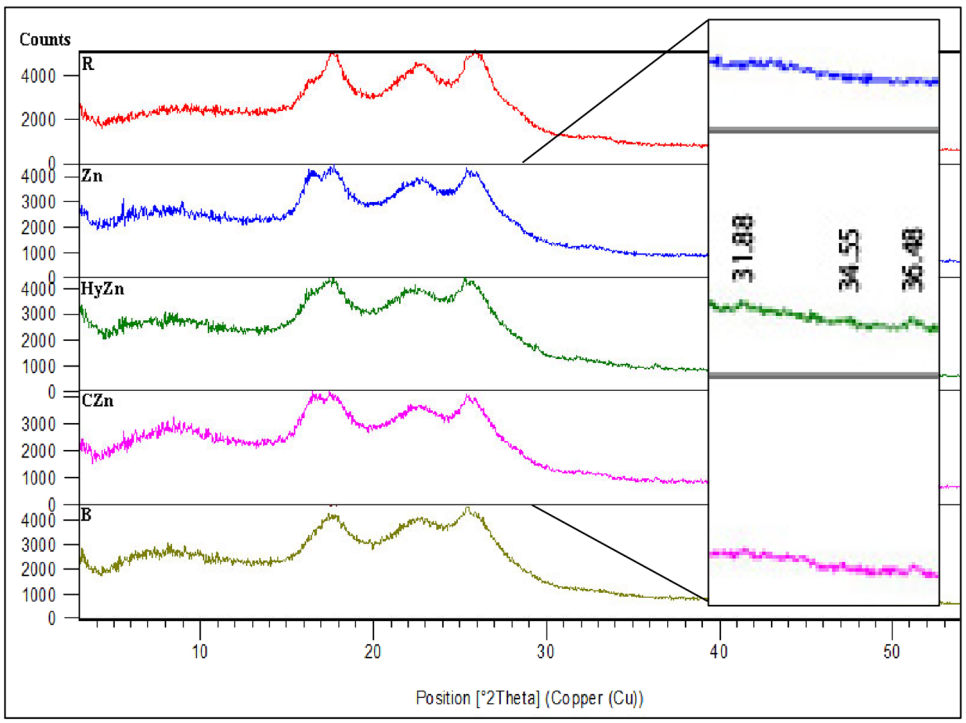

Fig. 5 XRD patterns of various samples

Table 2 Weight change of different samples

Experiments	1			2			3		
Samples	R	Zn	ZnP	Hy	HyZn	HyZnP	C	CZn	CZnP
Weight before treatment (g)	0.337	0.340	0321	0.328	0.335	0.307	0.316	0.328	0.311
Weight after treatment (g)	0.337	0.340	0.321	0.327	0.334	0.305	0.315	0.325	0.310
$\Delta W\%$	0.0	0.0	0.0	− 0.3	− 0.3	− 0.6	− 0.3	− 0.9	− 0.3

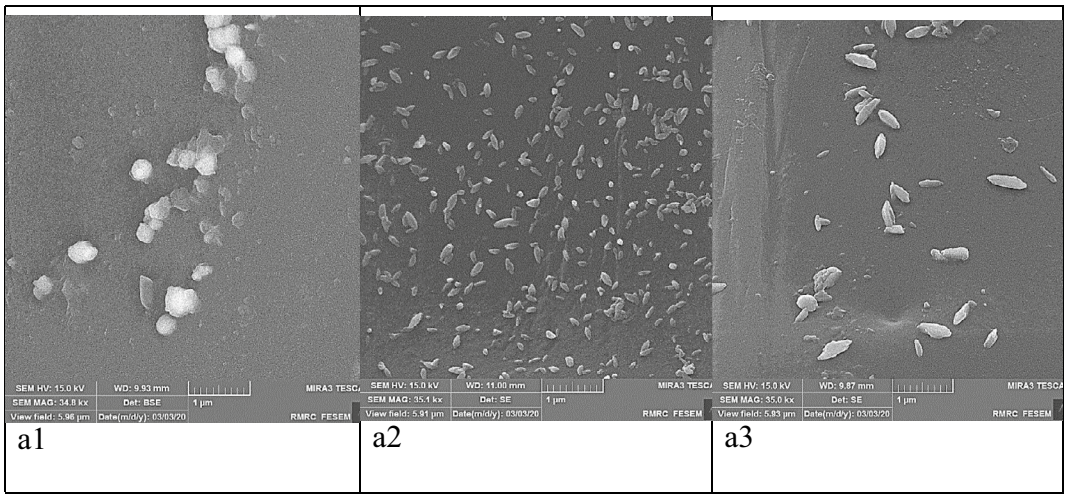

Fig. 6 FESEM images of a1) to a3) Zn, HyZn, and CZn samples in 35 kX

Also, the peak intensity of ZnO with a hexagonal structure in HyZn is higher than in other samples.

Weight change

The effect of synthesis, dyeing, and hydrolysis on PET fabric was investigated by calculating weight change during the processing with $\Delta W\%$ of 0.0 to − 0.9; here, 0.0 belongs to 1st experiment (R, Zn, and ZnP samples) with no alkali, and − 0.3, − 0.6 and − 0.9 is related to other samples, indicating breakage of ester chains in PET fabric, creation of oligomers, and additional low molar mass particles detached from the PET fabric, while hydrolysis is taken place. Table 2 demonstrates the weight of fabrics before and after simultaneous synthesis, hydrolysis, and dyeing.

Morphological studies

The synthesis of ZnO-NPs can be approved by FESEM images in Fig. 6. However, their shape and distribution are different due to the various synthesis conditions. The ZnO-NPs on the Zn sample are spherical with uneven distribution due to a lack of alkali. The smaller size with better distribution of ZnO-NPs can be observed on the samples treated in alkali media, such as HyZn with bead-like shape nanoparticles as the best sample. More concentration of alkali (pH = 10) led to bigger size nanoparticles such as CZn sample (Nair et al. 2009). The findings here are very similar to the others as the spherical shape is reported at a lower pH (6–7) and bead or rod shapes at a higher pH (10–12) (Wahab et al. 2009).

Influence of air plasma pre-treatment on dyeing of samples included ZnO-NPs

By using air plasma as a pre-treatment, the polyester fabric was activated, and cracks and pores formed on the surface can be seen on ZnP and HyZnP samples. ZnP showed agglomeration and uneven distribution of nanoparticles, and HyZnP showed a smaller with better distribution of ZnO-NPs. The shape of the nanoparticles is bead-like. The size of nanoparticles in CZnP is bigger with lower evenness. Figure 7 shows the distribution of particles on the pre-treated sample with air plasma. The size of zinc oxide nanoparticles is within 38–94 nm.

Color strength

Colorimetric properties of the fabrics, such as L^*, a^*, and b^*, were calculated based on AATCC test method 173–2006 in illuminant D65, CIE 10° standard observer, and large area view. To have an opaque view, samples were folded twice.

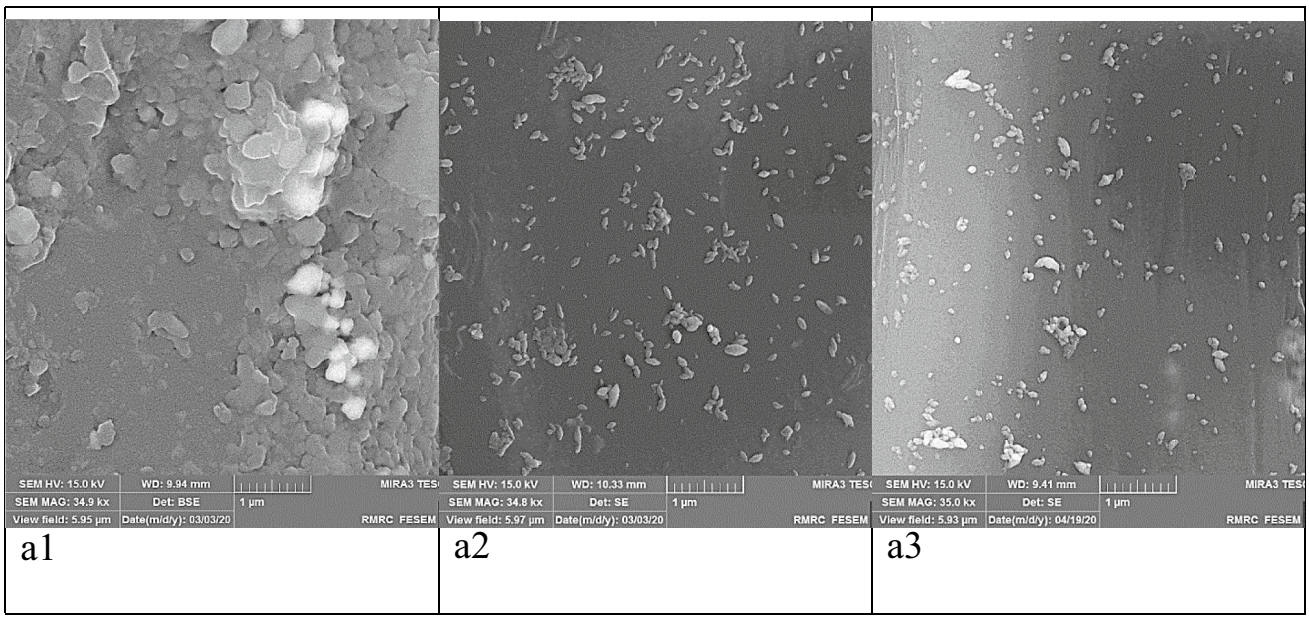

Fig. 7 FESEM images of a1) to a3) ZnP, HyZnP, and CZnP samples in 35 kX

Table 3 Colorimetric characteristics of the dyed samples included ZnO-NPs

Experiments	1			2			3		
Samples	R	Zn	ZnP	Hy	HyZn	HyZnP	C	CZn	CZnP
L*	37.6	38.2	37.2	40.1	37.0	37.1	38.0	38.5	38.5
a*	4.7	4.3	4.1	3.6	4.9	4.5	3.9	4.6	4.7
b*	− 39.9	− 39.6	− 38.5	− 39.0	− 40.1	− 39.4	− 38.8	− 40.3	− 40.2
K/S	3.13	3.73	4.14	3.63	4.07	4.35	3.51	3.91	4.22
Δ*E*	–	0.78	1.57	2.87	0.66	0.73	1.42	0.99	0.95
Absorbance	0.1	0.07	0.04	0.09	0.05	0.08	0.05	0.04	0

L*, b*, and a* are symbols for properties of color. Star (*) is part of their symbols. It doesn't mean definig somthingas asterisk

Table 3 signifies the colorimetric features of PET samples. Low *L** values specify a suitable color amount. Besides, the little positive values of *a** and large negative numbers of *b** suggested the combination of a little red and deep blue color, which exclusively approves the blue color of the used dye.

The color strength of treated samples was calculated using Kubelka–Munk Eq. 25:

$$K/S = \frac{(1-R)^2}{2R} \tag{25}$$

where *R*, *K*, and *S* stand for reflectance percentage, absorption coefficient, and scattering coefficient of dyes, respectively. The λ_{max} at which the absorbance was taken is 612 nm.

The dye diffusion into the fiber improves by lower crystallinity, and amorphous regions are better for penetration of the dye molecules (Zhao et al. 2014). Therefore, it seems that the crystallinity of treated samples was reduced due to hydrolysis and ZnO-NPs synthesis alongside air plasma pre-treatment. This may prepare a sufficient amorphous region for good dye uptake.

The *K*/*S* of various samples is shown in Table 3. The highest *K*/*S* is related to HyZnP with NaOH and ZnO-NPs pre-treated with air plasma. Other results signify the effects of synthesized ZnO-NPs or different alkalis. For instance, the lowest *K*/*S* is related to *R* without additive. Furthermore, the dyed sample with a carrier (CR) neither with alkali media and ZnO-NPs nor pre-treated with air plasma showed lower *K*/*S* (3.80) compared with other samples. The order of *K*/*S* values for different samples is:

HyZnP > CZnP > ZnP > HyZn > CZn > CR > Zn > Hy > C > R

This shows that the stronger alkali and zinc salt alongside air plasma pre-treatment leads to a stronger color. Further, alkali and zinc salt ended with high *K*/*S* values indicating the effect of alkali on the color strength compared with other

Table 4 The color fastness and related Δ*RGB* of various dyed samples included ZnO-NPs

Experiments	1			2			3		
Samples	R	Zn	ZnP	Hy	HyZn	HyZnP	C	CZn	CZnP
Washing Fastness	5	5	5	5	4–5	5	5	4–5	5
Δ*RGB*	8.0	8.5	4.5	1.8	12.6	6.6	6.4	14.1	7.4
Dry rubbing fastness	5	5	5	5	5	5	5	5	5
Δ*RGB*	8.0	8.5	4.5	1.9	2.6	6.6	6.4	4.0	7.4
Wet rubbing Fastness	4–5	5	5	4–5	5	4–5	5	4–5	5
Δ*RGB*	16.6	13.2	8.8	18.3	2.4	20.8	14.8	16.1	10.2
Light Fastness	7	7–8	8	6	8	7	7–8	8	8
Δ*RGB*	18.9	16.7	14.1	19.4	6.6	18.3	17.2	12.8	13.4

samples. In other words, carrier dyeing leads to more *K*/*S* compared with the raw or alkaline and Zn samples only.

Color fastness

One of the important factors in the usage of dyed textiles is calculating color fastness (Emam et al. 2014). The color fastness of samples was examined, and the outcomes are shown in Table 4. To be more precise Δ*RGB* of mentioned samples were calculated according to Eq. 26:

$$\Delta RGB = ((B_2 - B_1)^2 + (G_2 - G_1)^2 + (R_2 - R_1)^2)^{1/2} \quad (26)$$

The color fastness of 4–5 was recorded for HyZn and CZn, and 5 for other samples against washing, according to the grayscale, showed excellent washing fastness. The rubbing fastness of samples was also recorded sound results with a dry rubbing fastness of 5 for all tested samples, a wet rubbing fastness of 5 for most samples, and 4–5 for R, Hy, HyZnP, and CZn. The color fastness of samples against the light was also excellent. The result of 8 based on a blue scale for most samples (treated with ZnO-NPs) was recorded. Color fading in sunlight happens mainly by photo-degradation of the chemical structures of dyes. UV absorbers and antioxidants lead to a slight decrease in dye uptake and, in most cases, improve the light fastness (Li et al. 2018).

The synthesis of ZnO-NPs along with dyeing acted as UV absorbers improved the light fastness (Nourbakhsh et al. 2018). The dye molecules interacted with Zn^{2+}, and reactive groups of PET formed the organo-metallic complexes that prevented the degradation of dyes through the radicals produced from ZnO-NPs under the lights. As evidenced, light fastness results indicated no changes in the sample color after 30 h under UV irradiation.

Also, discoloration of CI Reactive Black 5 in an aqueous solution was carried out by adding a piece of nano-titanium dioxide-treated fabric into the dye solution under UV-A irradiation. By using UV spectra, complete discoloration of the dye was achieved (Montazer and Hashemikia 2012). This shows that the dyed treated fabric can be applied for discoloration of free dye in effluent through a photocatalysis mechanism.

ZnO content

In order to find the changes in the ZnO-NPs content of PET fabric, five samples were put in a furnace for 3 h at 600 ℃ to analyze the weight changes. The first and second samples were raw and synthesized/dyed fabric (HyZn), and the third, fourth, and fifth samples were the second samples after washing, rubbing, and lighting. It was revealed that the rubbing fastness caused the most removal of ZnO-NPs with a reduction of 1.7% while washing reduced by 1.2% and lighting declined the least value of 1%. Thus, it seems that the simultaneous synthesis and dyeing of PET fabric has no significant influence on the ZnO-NPs content of the fabric.

Antibacterial activities

The antibacterial activities of treated samples were tested using a Gram-positive bacterium; *S. aureus,* and a Gram-negative one; *E. coli*. The samples were placed on agar plates containing the mentioned bacteria. After incubation in the dark for 24 h, the grown bacteria of both types filled the untreated sample; however, the growth of bacteria was inhibited for *S. aureus* for some treated samples. On the other hand, no inhibition of bacteria growth was found against *E. coli,* similar to the previous report (Ashraf et al. 2014) (Fig. 8.).

The Zn (92.5%), ZnP (76%), and HyZn (99%) approved the inhibition of *S. aureus* growth, according to Fig. 9. However, R and CZn failed to show the inhibition of bacteria growth. Both physical and chemical interactions

caused inhibition of bacteria growth. The zeta potential of ZnO is + 24 mV at pH = 7.2, while the bacteria's surface is negatively charged. Therefore, the attachment of bacteria to the ZnO surface can be due to electrostatic interactions (Du et al. 2021). Also, penetration of the tiny ZnO-NPs to the cell membranes leads to their fragmentation and malfunctioning (Applerot et al. 2009) and causes bacteria death. The production of reactive oxygen species (ROS) is the second major factor, which includes $^{\cdot}OH$, H_2O_2, and O_2^{2}, which lead to cell death resulting from damaging DNA, cell membranes, and cellular proteins. Hydroxyl radical ($^{\cdot}OH$) is the most sensitive oxygen radical and reacts very rapidly with approximately all molecules in living cells (Moody and Hassan 1982). Such reactions may be recombined with two OH radicals to create hydrogen peroxide (H_2O_2), a weaker oxidizer

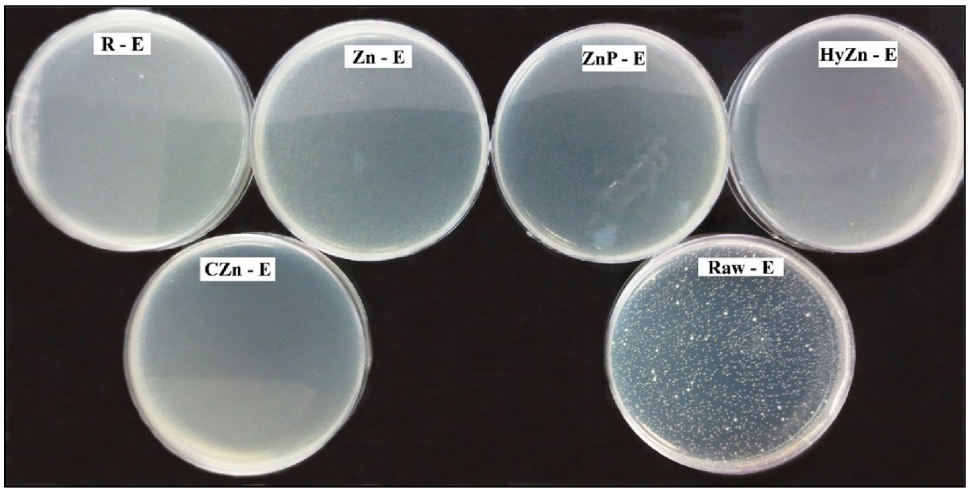

Fig. 8 Antibacterial properties of treated and untreated samples against *E. coli*

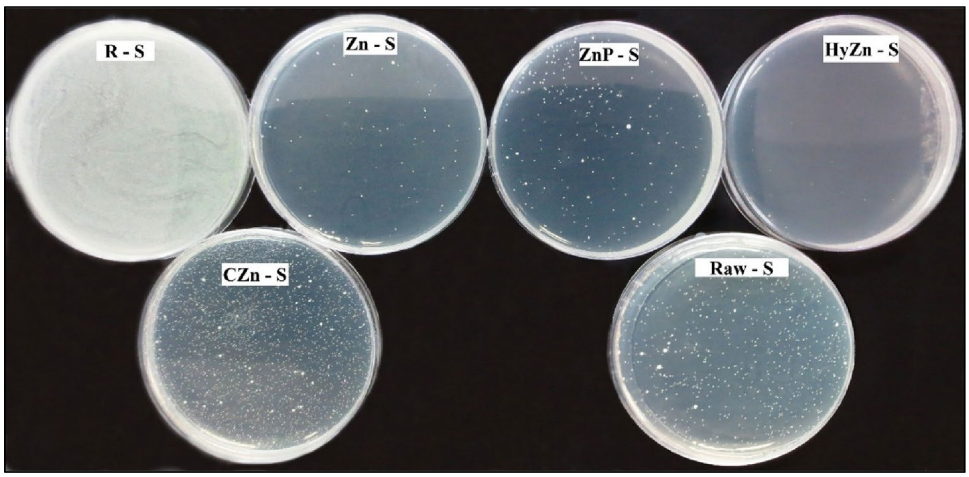

Fig. 9 Antibacterial properties of treated and untreated samples against *S. aureus*

Table 5 Cell viability of various dyed samples containing ZnO-NPs

570 nm	R	Zn	ZnP	HyZn	CZn	Raw	Control
A	0.306	0.017	0.156	0.012	0.013	0.149	0.127
B	0.382	0.040	0.143	0.019	0.025	0.221	0.143
C	0.331	0.030	0.170	0.006	0.012	0.157	0.163
Mean	0.339	0.029	0.156	0.012	0.016	0.175	0.144
Cell viability %	235.4	20.1	108.3	8.3	11.1	121.5	–

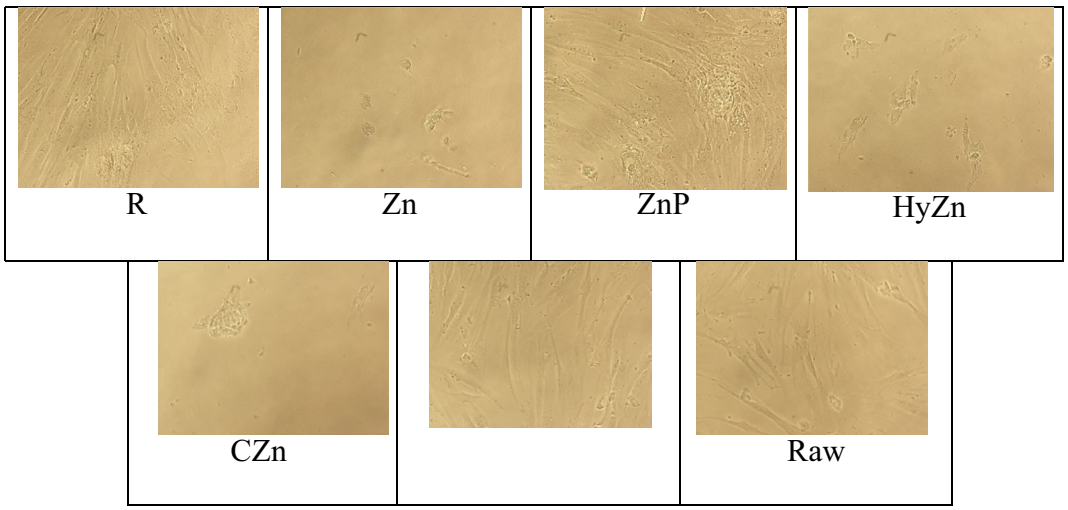

Fig. 10 Cell growth pictures of various dyed samples included ZnO-NPs

that causes cell destruction by hydroxyl radicals formed through the Fenton reaction (Hassan and Fridovich 1979).

The smaller ZnO-NPs with a better distribution on the PET surface make more bacteria growth inhibition (HyZn).

The large surface area of the nanoparticles improves diffusion into the cell membrane. The agglomerated particles with bigger size and uneven distribution on the plasma pre-treated sample (ZnP) were directed to lower antibacterial activity compared to the sample (Zn) without pre-treatment. Moreover, weaker alkali in CZn resulted in the growth of both bacteria. *R* sample with no ZnO-NPs on the surface caused bacterial growth.

Cytotoxicity results

According to ISO 10993-5, mean cell viability over 70% in a textile makes a good compatible substrate with human dermal fibroblasts (Montazer et al. 2015). The related results are reported in Table 5.

The cell growth pictures of treated fabrics are demonstrated in Fig. 10. Based on Table 5, R, ZnP, and raw samples indicated acceptable cell viability results. It is also revealed that the dye alone has a very interesting outcome for human body skin. In comparing the mentioned three samples with those samples indicating good antibacterial effects (i.e., Zn, ZnP, and HyZn), it can be considered that ZnP (air plasma pre-treated) is presented in both groups, which can be proposed as a safe antibacterial sample for straight use, especially in medical applications. This can be related to the use of safe, dry processing of air plasma along with biocidal materials of ZnO-NPs that reduce the toxicity of the final product (Montazer et al. 2015).

Furthermore, the air plasma pre-treatment increases the ZnO-NPs agglomeration (Fig. 7-a1), and the bigger size

Table 6 Mechanical properties of various dyed samples included ZnO-NPs

Experiments	1			2			3				
Samples	R	Zn	ZnP	Hy	HyZn	HyZnP	C	CZn	CZnP	Control	Raw
Breaking tenacity (MPa)	57.5	60.9	58.7	57.4	57.7	58	57.9	58.7	58.6	58.3	57.5
C.V.%	3.55	1.49	2.62	3.18	3.24	5.63	3.37	4.57	5.02	2.88	1.02
Elongation %	41.11	47.78	50.28	45.28	46.94	50.27	45.28	46.67	50.00	28.32	23.61
C.V.%	2.53	2.60	2.53	2.13	2.05	2.47	2.13	3.09	5.77	3.11	2.04
Bending length (cm)	1.8	1.6	1.6	1.7	1.4	1.6	1.6	1.6	1.6	1.5	2.7
C.V.%	2.73	2.68	2.15	2.34	2.17	2.29	2.93	2.88	2.61	2.59	2.37
Crease recovery angle (°)	155	175	161	169	162	162	163	150	166	157	110
C.V.%	1.89	2.84	2.95	2.78	3.21	2.41	1.82	1.46	3.11	2.65	2.34
Air permeability ($cm^3/s/cm^2$)	68.8	66.0	95.6	77.6	112.4	78.6	77.2	95.4	90.6	71.6	63.2
C.V.%	3.71	3.23	2.89	2.44	1.96	2.39	2.27	3.12	1.46	1.97	1.74

particles (agglomerated) decrease the toxicity of ZnO-NPs that can also be considered as the diminished gathering of intracellular Zn ions (Fang et al. 2017). Thus, the air plasma pre-treatment helps to diminish the adverse influence of ZnO-NPs on the safety of the treated samples.

Mechanical properties

The dyed ZnO-NPs synthesized samples made changes in the physical structures of the samples.

Mechanical properties of the treated samples, including raw and control (raw fabric treated with distilled water at 130 °C for 1 h) samples, are summarized in Table 6.

Zn, ZnP, CZn, and CZnP samples had the best results regarding the breaking tenacity. The formation and growth of cracks throughout the tensile measurement were prolonged (Allahyarzadeh et al. 2013); however, the synthesized ZnO-NPs caused acceptable breaking tenacity presumably because of the filling of the formed pits (especially for the pre-treated samples); thus, mechanical load distributed uniformly on the surface of the fabric (Harifi and Montazer 2014b). Moreover, the extent of alkali hydrolysis for the synthesized ZnO-NPs samples was less than alkali-hydrolyzed samples, as part of alkali consumed with zinc salt to form zinc hydroxide for the fabrication of ZnO-NPs. The breaking tenacity of other samples demonstrated little difference with each other.

ZnP, HyZnP, and CZnP samples have the highest elongation percentage, indicating that air plasma pre-treatment produces appropriate mechanical results in addition to other beneficial and safe effects. Conversely, the control and raw samples had the lowest elongation percentage.

The bending lengths of all samples are lower than the raw sample as a result of ZnO-NPs synthesis and hydrolysis of PET. This leads to a soft handle with lower rigidity (Allahyarzadeh et al. 2013). The treated samples with enhanced flexibility indicated a higher wrinkle reclamation angle. The crease recovery angle of 110° was recorded for the raw rigid sample; however, all treated samples showed a higher crease recovery angle. This may be because locally producing ZnO-NPs on PET fabric allows penetration of nanoparticles into fabric structure formed nano-cross-linking between the PET chains. Thus, with an external force, fabric deformation occurs; consequently, nano-cross-linked chains try to restore their original state, leading to a higher crease recovery angle (Memon et al. 2016; Shady et al. 2012). In addition, the air plasma pre-treated samples may cause chemical cross-linking due to the formation of free radicals attributed to the air plasma pre-treatment or oligomers. This may produce a very thin cross-linked layer on the surface leading to an increased crease recovery angle (Bhat and Benjamin 1989).

Air permeability measures the proportion of airflow transient vertically along a definite part in an arranged air pressure differential among the two sides of textile fabrics. Many features, such as temperature and pressure, polymer nature and morphology, penetrant molecule dimension and activity, are important in the permeability of polymers (Peterlin 1975). In this study, the air permeability of treated samples improved noticeably as more chain flexibility (which was approved by the crease recovery angle) increased the penetrant diffusivity or permeability (Sorrentino et al. 2012). Further, alkaline hydrolysis developed permeability since fiber diameter and thickness diminished, and hydrophilic groups were introduced after alkali hydrolysis (Han et al. 2016). Likewise, using air plasma as a pre-treatment makes pores and cracks promote permeability. At last, the permeability of a polymer can be affected by chain orientation and in situ production of ZnO-NPs that led to the microvoids' development (Sorrentino et al. 2012; Tabatabaei et al. 2008). In this process, by in situ synthesis of ZnO-NPs, removing loose fibers from the fabric surface can effortlessly pass air through the fabric's pores (Talebi and Montazer 2020), as the air permeability is directly related to the textile porosity (Lee and Obendorf 2001).

Resistance in alkali media

Polyester quickly decomposes in an alkaline solution of sodium hydroxide (NaOH) through more treatment time and NaOH above 20%, and in lower concentrations, the fabric loses its weight (Rezaie and Montazer 2017). This occurs through the breakage of PET chains by the NaOH attack on the ester bond of fabric, resulting in hydroxyl end groups. The effect of alkali hydrolysis was studied on dyed, and ZnO-NPs synthesized PET fabrics. Separate baths containing a 50 mL solution of 20% (w/v) sodium hydroxide were prepared, and samples of the same weight (0.1 g) were put in them, boiling for 55 min. All solution's color was clear at first; however, after 20 min, the raw sample was entirely decomposed and transformed into a white solution. Other colored samples were gradually torn into small blue pieces and then turned into dark and black colored pieces and finally formed a white layer of semi-hard NaOH residue with some parts of the samples. These changes were first started by Zn and HyZnP (35 min) and then R, ZnP, and Hy (42 min). This was prolonged for HyZn, C, CZn, and CZnP for 55 min to decompose incompletely. The PET fabric synthesized and hydrolyzed with Na_2CO_3 showed more resistance against alkali media of NaOH than other samples.

This achievement may have some causes; the first nano-cross-linking amid the chemical structure due to the production of ZnO-NPs and hydrolysis of PET fabric in

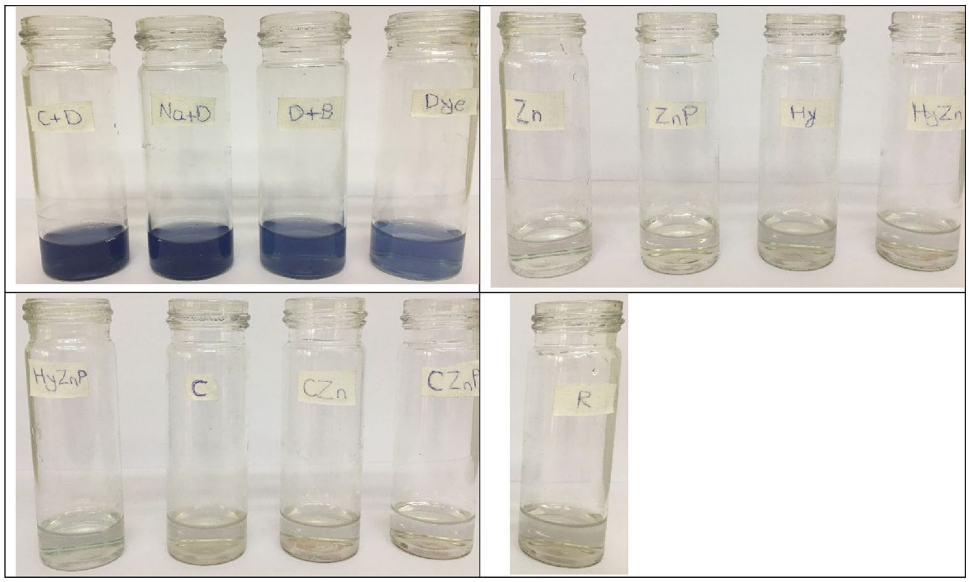

Fig. 11 Pictures of the remaining dye bath of various dyed samples included ZnO-NPs

alkali media occurred, and separation of PET chains was avoided. Second, using C.I. Disperse Blue 19 with amine groups can influence hydrolysis; the mechanism is much similar to that of ester hydrolysis; however, it is much slower. In addition, the separation of the hydrolyzed parts from the backbone can be prevented by cross-linking the separated oligomers with polymeric chains. At last, in situ production of ZnO-NPs and distribution on the fabric surface reduced the essential ester bonds on the PET for hydroxyl anion nucleophilic attack. Hence, the synthesized samples presented higher stability in a concentrated alkali media of NaOH and retarded the hydrolysis of the synthesized PET (Rezaie and Montazer 2017).

Effluent studies

UV–Vis spectroscopy was used to consider the remaining dye molecules in different synthesized and dyed bath effluent. It seems that the synthesis and dyeing in one step can be mentioned as a clean method for producing the desired color alongside multifunctional properties. Few dye molecules remained in the dye bath, particularly in the simultaneous synthesis of ZnO-NPs, as confirmed by the UV–Vis results. The remaining synthesized ZnO-NPs as nano-photocatalysts can also degrade effluent's dye under sunlight (Jamil et al. 2020). More residual dye molecules remained in the dye bath without ZnO-NPs (R and Hy samples) even though the total dye remaining was very low (the UV absorbance of all samples was between 0 and 0.1). This shows that the introduced process is facile, cost-effective, and environmentally friendly due to the very low remaining chemical compounds. The results of UV absorbance are displayed in Table 3.

Further, to study the effect of alkaline itself on the color of the dye, three samples were made, including dye solution and NaOH (Na + D), dye with Na_2CO_3 (C + D), and dye solution in boil condition (D + B) that were treated in the same condition of dyeing. According to UV absorbance, alkali media has a low effect on the color of the dye's chemical structure. However, the minor dye solubility at higher pH causes an important improvement in dye absorption through the growing attraction of the dye to the PET fabric. The decomposition of dyes is related to the substituents of dye and functional groups in their chemical structure. For instance, most of the azo dyes with functional groups of amide, cyano, and ester decompose in alkali media must be used at pH = 4–5 (Shakra et al. 1979). The used dye in this work has an anthraquinone structure that is stable in alkali media.

The sample without alkali or ZnO-NPs showed clear effluent because of the presence of polyester fabric in the bath to the uptake of dye. However, more dye uptake occurred in other samples due to the influence of alkaline and ZnO-NPs. Also, the UV–Vis spectra revealed that more dye molecules remained in the baths without ZnO-NPs.

The pictures of the remaining baths presented in Fig. 11 show a clear solution with no color confirmed by the UV–Vis spectra.

Finally, the outcomes are summarized in Fig. 12, as the polyester fabric demonstrates outstanding results with multifunctional properties.

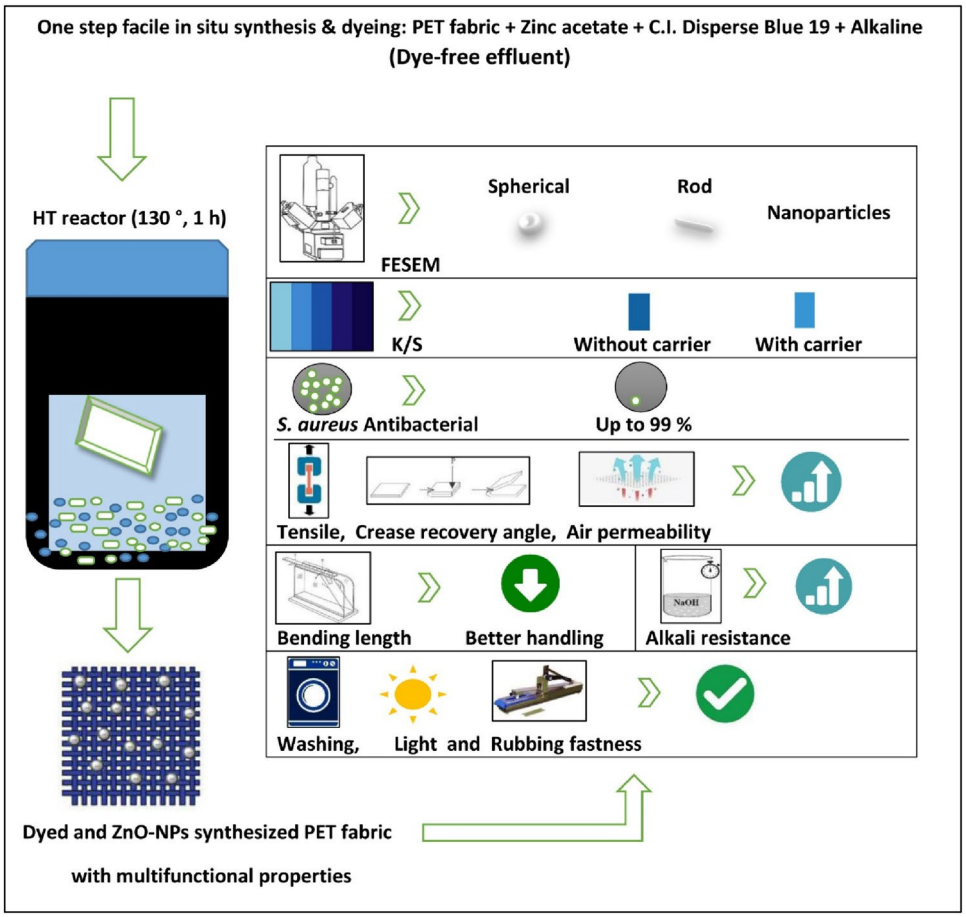

Fig. 12 Schematic of the outcomes of one-step facile ZnO-NPs synthesis and dyeing of PET fabric

Conclusion

Here, an eco-friendly one-step route for ZnO-NPs synthesizing and dyeing of the raw and air plasma pre-treated polyester fabrics was introduced using Disperse Blue 19 and zinc acetate with and without alkaline. Dye-free effluent was achieved as a clean way of this concurrent process without hazardous colored effluent of conventional disperse dyeing of PET fabric. The lack of carrier in this procedure and the use of zinc salt had combinatory results, which led to higher color strength besides clean dyeing effluent reducing processing steps to one and resulting in much lower energy, time, and production cost. Furthermore, this can be used on the industrial scale to preserve many of the mentioned achievements considering the extensive application of PET fabric.

The synthesis of ZnO-NPs was proved by FESEM images and FT-IR patterns, as the HyZn sample showed the smallest particles with the best distribution. Further, the color strength of samples (*K*/*S*) indicated better strength between the synthesized ZnO-NPs samples. In addition, the HyZn sample was designated the best antibacterial effects on *S. aureus*; however, considering the cell cytotoxicity, the ZnP sample was the acceptable sample with safe antibacterial properties for direct application in medical purposes. Additionally, through in situ synthesis alongside dyeing, the tensile strength, crease recovery angle, and air permeability improved, and bending length declined to propose better handling. These show the capability of the final product to be used as a fabric with various functionalities in multi-purpose applications. Besides, the color fastness of the samples against washing, rubbing, and light revealed reasonable stability of the accomplished synthesis and dyeing. At last, several samples showed more resistance against alkali media a good achievement for new applications. All in all, the simple, clean, cost-effective, and industrially scalable route is recommended for simultaneous dyeing and finishing of PET fabric to obtain multi-functional features. It was proposed that similar procedure may applied on polyester fabric with different dyes to simplify and lower the cost of both dyeing the fabrics and synthesizing metal oxides. Furthermore, it is recommended that this process can be scaled up for more outstanding accomplishments.

Author contributions Seyed Mohammad Taher Shahin helped in data curation, writing—original draft preparation, investigation. Majid Montazer contributed to supervision, conceptualization, reviewing and editing, and validation. Mahnaz Mahmoudirad was involved in data curation, visualization, validation.

Funding The authors have not disclosed any funding.

Data availability Enquiries about data availability should be directed to the authors.

Declarations

Conflict of interest The authors have not disclosed any competing interests.

References

Afshari S, Montazer M, Harifi T, Mahmoudi Rad M (2019) A coloured polyester fabric with antimicrobial properties conferred by copper nanoparticles. Color Technol 135(6):427–438. https://doi.org/10.1111/cote.12430

Ahmed N, Nassar S, El-Shishtawy MR (2020) A novel green continuous dyeing of polyester fabric with excellent color data. Egypt J Chem 63(1):1–14. https://doi.org/10.21608/ejchem.2020.22055.2318

Alias SS, Mohamad AA (2014) Synthesis of zinc oxide by sol-gel method for photoelectrochemical cells. Springer, Singapore, pp 41–50. https://doi.org/10.1007/978-981-4560-77-1

Allahyarzadeh V, Montazer M, Nejad NH, Samadi N (2013) In situ synthesis of nano silver on polyester using NaOH/Nano TiO_2. J Appl Polym Sci 129(2):892–900. https://doi.org/10.1002/app.38907

Andreola F, Barbieri L, Bondioli F, Cannio M, Ferrari AM, Lancellotti I (2008) Synthesis of chromium containing pigments from chromium galvanic sludges. J Hazard Mater 156(1–3):466–471. https://doi.org/10.1016/j.jhazmat.2007.12.075

Anna K, Nina P, Yuri K, Meinhard M, Werner Z, Aharon G (2008) Coating zinc oxide submicron crystals on poly (methyl methacrylate) chips and spheres via ultrasound irradiation. Ultrason Sonochem 15(5):839–845. https://doi.org/10.1016/j.ultsonch.2007.10.011

Applerot G, Lipovsky A, Dror R, Perkas N, Nitzan Y, Lubart R, Gedanken A (2009) Enhanced anti-bacterial activity of nanocrystalline ZnO due to increased ROS-mediated cell injury. Adv Func Mater 19(6):842–852. https://doi.org/10.1002/adfm.200801081

Arcoria A, Longo ML, Parisi G (1985) Effects of the phenol on the dyeing of polyester fibre with some disperse azo-dyes. Dyes Pigm 6(2):155–161. https://doi.org/10.1016/0143-7208(85)80014-0

Ashraf M, Dumont F, Campagne C, Champagne P, Perwuelz A, Leriche A, Chihib NE (2014) Development of anti-bacterial polyester fabric by growth of ZnO nanorods. J Eng Fibers Fabr 9(1):155892501400900100. https://doi.org/10.1177/155892501400900103

Bhat NV, Benjamin YN (1989) Modification of polyester by DC plasma: effect on fine structure and textile properties. IJFTR. 14:1–8. http://nopr.niscpr.res.in/handle/123456789/32634

Bhuiyan MR, Ali A, Islam A, Hannan MA, Kabir SF, Islam MN (2018) Coloration of polyester fiber with natural dye henna (*Lawsonia inermis* L.) without using mordant: a new approach towards a cleaner production. Fash Text. 5(1):2. https://doi.org/10.1186/s40691-017-0121-1

Choudhury AR (2006) Textile preparation and dyeing. Science Publishers, New Delhi

Chrysler LP (1990) Methods of test for color fastness of textiles and leather. Bradf Lond UK, pp. 89–94

Dave H, Ledwani L, Chandwani N, Desai BD, Nema SK (2014) Surface activation of polyester fabric using ammonia dielectric barrier discharge and improvement in colour depth. Indian J Fibre Text Res (IJFTR) 39(3):274–281

Du H, Yuan F, Huang S, Li J, Zhu Y (2004) A new reaction to ZnO nanoparticles. Chem Lett 33(6):770–771. https://doi.org/10.1246/cl.2004.770

Du M, Zhao W, Ma R, Xu H, Shan C, Liu K, Zhuang J, Jiao Z (2021) Visible-light-driven photocatalytic inactivation of *S. aureus* in aqueous environment by hydrophilic zinc oxide (ZnO) nanoparticles based on the interfacial electron transfer in *S. aureus*/ZnO composites. J Hazard Mater 418:126013. https://doi.org/10.1016/j.jhazmat.2021.126013

Ebrahimi I, Kiumarsi A, Gashti MP, Rashidian R, Norouzi MH (2011) Atmospheric-air plasma enhances coating of different lubricating agents on polyester fiber. Eur Phys J Appl Phys 56(1):10801

Emam HE, Mowafi S, Mashaly HM, Rehan M (2014) Production of anti-bacterial colored viscose fibers using in situ prepared spherical Ag nanoparticles. Carbohyd Polym 110:148–155. https://doi.org/10.1016/j.carbpol.2014.03.082

Fang X, Jiang L, Gong Y, Li J, Liu L, Cao Y (2017) The presence of oleate stabilized ZnO nanoparticles (NPs) and reduced the toxicity of aged NPs to Caco-2 and HepG2 cells. Chem Biol Interact 278:40–47. https://doi.org/10.1016/j.cbi.2017.10.002

Ghule K, Ghule AV, Chen BJ, Ling YC (2006) Preparation and characterization of ZnO nanoparticles coated paper and its antibacterial activity study. Green Chem 8(12):1034–1041. https://doi.org/10.1039/B605623G

Gorenšek M, Gorjanc M, Bukošek V, Kovač J, Petrović Z, Puač N (2010) Functionalization of polyester fabric by Ar/N_2 plasma and silver. Text Res J 80(16):1633–1642. https://doi.org/10.1177/0040517510365951

Han MS, Park Y, Park CH (2016) Development of superhydrophobic polyester fabrics using alkaline hydrolysis and coating with fluorinated polymers. Fibers Polym 17(2):241–247. https://doi.org/10.1007/s12221-016-5693-7

Harifi T, Montazer M (2013) Free carrier dyeing of polyester fabric using nano TiO_2. Dyes Pigm 97(3):440–445. https://doi.org/10.1016/j.dyepig.2013.01.015

Harifi T, Montazer M (2014a) In situ synthesis of iron oxide nanoparticles on polyester fabric utilizing color, magnetic, antibacterial and sono-Fenton catalytic properties. J Mater Chem B 2(3):272–282. https://doi.org/10.1039/C3TB21445A

Harifi T, Montazer M (2014b) Photo-, bio-, and magneto-active colored polyester fabric with hydrophobic/hydrophilic and enhanced mechanical properties through synthesis of TiO_2/Fe_3O_4/Ag nanocomposite. Ind Eng Chem Res 53(3):1119–1129. https://doi.org/10.1021/ie403052m

Hasnidawani JN, Azlina HN, Norita H, Bonnia NN, Ratim S, Ali ES (2016) Synthesis of ZnO nanostructures using sol-gel method. Procedia Chem 19:211–216. https://doi.org/10.1016/j.proche.2016.03.095

Hassan HM, Fridovich I (1979) Paraquat and *Escherichia coli* Mechanism of production of extracellular superoxide radical. J Biol Chem 254(21):10846–10852

ISO, B. (1999) 10993-5: biological evaluation of medical devices. Tests in vitro Cytotox

Jamil A, Bokhari TH, Javed T, Mustafa R, Sajid M, Noreen S, Zuber M, Nazir A, Iqbal M, Jilani MI (2020) Photocatalytic degradation of disperse dye Violet-26 using TiO_2 and ZnO nanomaterials and process variable optimization. J Market Res 9(1):1119–1128. https://doi.org/10.1016/j.jmrt.2019.11.035

Kerkeni A, Behary N, Perwuelz A, Gupta D (2012) Dyeing of woven polyester fabric with curcumin: effect of dye concentrations and surface pre-activation using air atmospheric plasma and ultraviolet excimer treatment. Color Technol 128(3):223–229. https://doi.org/10.1111/j.1478-4408.2012.00367.x

Küçük M, Öveçoğlu ML (2018) Surface modification and characterization of polyester fabric by coating with low temperature synthesized ZnO nanorods. J Sol-Gel Sci Technol 88(2):345–358. https://doi.org/10.1007/s10971-018-4817-5

Lee S, Obendorf SK (2001) A statistical model to predict pesticide penetration through nonwoven chemical protective fabrics. Text Res J 71(11):1000–1009. https://doi.org/10.1177/004051750107101111

Li R, Jiang Z, Chen F, Yang H, Guan Y (2004) Hydrogen bonded structure of water and aqueous solutions of sodium halides: a Raman spectroscopic study. J Mol Struct 707(1–3):83–88. https://doi.org/10.1016/j.molstruc.2004.07.016

Li WJ, Shi EW, Zhong WZ, Yin ZW (1999) Growth mechanism and growth habit of oxide crystals. J Cryst Growth 203(1–2):186–196. https://doi.org/10.1016/S0022-0248(99)00076-7

Li C, Xiao H, Wang X, Zhao T (2018) Development of green waterborne UV-curable vegetable oil-based urethane acrylate pigment prints adhesive: preparation and application. J Clean Prod 180:272–279. https://doi.org/10.1016/j.jclepro.2018.01.193

Memon H, Yasin S, Khoso NA, Memon S (2016) Study of wrinkle resistant, breathable, anti-UV nanocoated woven polyester fabric. Surf Rev Lett 23(03):1650003. https://doi.org/10.1142/S0218625X16500037

Mirjalili M, Karimi L (2013) The impact of nitrogen low temperature plasma treatment upon the physical-chemical properties of polyester fabric. J Text Inst 104(1):98–107. https://doi.org/10.1080/00405000.2012.697309

Mohammadi M, Karimi L, Mirjalili M (2016) Simultaneous synthesis of nano ZnO and surface modification of polyester fabric. Fibers Polym 17(9):1371–1377. https://doi.org/10.1007/s12221-016-6497-5

Montazer M, Dastjerdi M, Azdaloo M, Rad MM (2015) Simultaneous synthesis and fabrication of nano Cu_2O on cellulosic fabric using copper sulfate and glucose in alkali media producing safe bio-and photoactive textiles without color change. Cellulose 22(6):4049–4064. https://doi.org/10.1007/s10570-015-0764-2

Montazer M, Hashemikia S (2012) Textile with immobilised nano titanium dioxide for repeated discoloration of CI Reactive Black 5 under UV-A. Color Technol 128(5):403–409. https://doi.org/10.1111/j.1478-4408.2012.00394.x

Moody CS, Hassan HM (1982) Mutagenicity of oxygen free radicals. Proc Natl Acad Sci 79(9):2855–2859

Morent R, De Geyter N, Verschuren J, De Clerck K, Kiekens P, Leys C (2008) Non-thermal plasma treatment of textiles. Surf Coat Technol 202(14):3427–3449

Nair S, Sasidharan A, Rani VD, Menon D, Nair S, Manzoor K, Raina S (2009) Role of size scale of ZnO nanoparticles and microparticles on toxicity toward bacteria and osteoblast cancer cells. J Mater Sci Mater Med 20(1):235. https://doi.org/10.1007/s10856-008-3548-5

Nourbakhsh S, Montazer M, Khandaghabadi Z (2018) Zinc oxide nano particles coating on polyester fabric functionalized through alkali treatment. J Ind Text 47(6):1006–1023. https://doi.org/10.1177/1528083716657819

Nunn DM (ed) (1979) The dyeing of synthetic-polymer and acetate fibres. Dyers Company Publications Trust, London. https://doi.org/10.1051/epjap/2011100511

Oskam G (2006) Metal oxide nanoparticles: synthesis, characterization and application. J Sol-Gel Sci Technol 37(3):161–164. https://doi.org/10.1007/s10971-005-6621-2

Osman DAM, Mustafa MA (2015) Synthesis and characterization of zinc oxide nanoparticles using zinc acetate dihydrate and sodium hydroxide. J Nanosci Nanoeng 1(4):248–251

Peterlin A (1975) Dependence of diffusive transport on morphology of crystalline polymers. J Macromol Sci Part B Phys 11(1):57–87. https://doi.org/10.1080/00222347508217855

Poortavasoly H, Montazer M (2014) Functional polyester fabric through simultaneous aminolysis and nano ZnO synthesis. J Ultrafine Grained Nanostruct Mater 47(2):113–119. https://doi.org/10.7508/jufgnsm.2014.02.008

Poortavasoly H, Montazer M, Harifi T (2014) Simultaneous synthesis of nano silver and activation of polyester producing higher tensile strength aminohydroxylated fiber with antibacterial and hydrophilic properties. RSC Adv 4(86):46250–46256. https://doi.org/10.1039/C4RA04835K

Raffaele-Addamo A, Riccardi C, Selli E, Barni R, Piselli M, Poletti G, Orsini F, Marcandalli B, Massafra MR, Meda L (2003) Characterization of plasma processing for polymers. Surf Coat Technol 174:886–890

Rezaie AB, Montazer M (2017) Amidohydroxylated polyester with biophotoactivity along with retarding alkali hydrolysis through in situ synthesis of Cu/Cu_2O nanoparticles using diethanolamine. J Appl Polym Sci. https://doi.org/10.1002/app.44856

Rezaie AB, Montazer M, Rad MM (2017) A cleaner route for nano-colouration of wool fabric via green assembling of cupric oxide nanoparticles along with anti-bacterial and UV protection properties. J Clean Prod 166:221–231. https://doi.org/10.1016/j.jclepro.2017.08.046

Samanta KK, Jassal M, Agrawal AK (2009) Improvement in water and oil absorbency of textile substrate by atmospheric pressure cold plasma treatment. Surf Coat Technol 203(10–11):1336–1342. https://doi.org/10.1016/j.surfcoat.2008.10.044

Shady KE, Michael MN, Shimaa HA (2012) Effects of zinc oxide nanoparticles on the performance characteristics of cotton, polyester and their blends. In: AIP conference proceedings, vol 1459, no. 1. American Institute of Physics, pp 356–359

Shakra S, Hanna HL, Hebeish A (1979) Effect of pH control on dyeing of polyester materials with disperse dyes. Die Angew Makromol Chem Appl Macromol Chem Phys 75(1):53–62. https://doi.org/10.1002/apmc.1979.050750104

Singh NL, Qureshi A (2005) N. shah, AK Rakshit, S. Mukherjee, A. Tripathi and DK Avasthi. Radiation Measurements, 40:746–750. https://doi.org/10.1016/j.radmeas.2005.01.014

Sorrentino A, Gorrasi G, Vittoria V (2012) Permeability in clay/polyesters nano-biocomposites. In: Environmental silicate nano-biocomposites. Springer, London, pp 237–264. https://doi.org/10.1007/978-1-4471-4108-2_9

Tabatabaei SH, Carreau PJ, Ajji A (2008) Microporous membranes obtained from polypropylene blend films by stretching. J Membr Sci 325(2):772–782. https://doi.org/10.1016/j.memsci.2008.09.001

Talebi S, Montazer M (2020) Denim fabric with flame retardant, hydrophilic and self-cleaning properties conferring by in-situ synthesis of silica nanoparticles. Cellulose 27:6634–6661

Uekawa N, Yamashita R, Wu YJ, Kakegawa K (2004) Effect of alkali metal hydroxide on formation processes of zinc oxide crystallites from aqueous solutions containing Zn $(OH)_4^{2-}$ ions. Phys Chem Chem Phys 6(2):442–446. https://doi.org/10.1039/B310306D

Wahab R, Ansari SG, Kim YS, Song M, Shin HS (2009) The role of pH variation on the growth of zinc oxide nanostructures. Appl Surf Sci 255(9):4891–4896. https://doi.org/10.1016/j.apsusc.2008.12.037

Wahab HA, Salama AA, El-Saeid AA, Nur O, Willander M, Battisha IK (2013) Optical, structural and morphological studies of (ZnO) nano-rod thin films for biosensor applications using sol

gel technique. Results Phys 3:46–51. https://doi.org/10.1016/j.rinp.2013.01.005

Yaman N, Özdogan E, Kocum İC, Ayhan H, Öktem T, Seventekin N (2009) Improvement surface properties of polypropylene and polyester fabrics by glow discharge plasma systemunder atmospheric condition. J Text Appar TekstilveKonfeksiyon 19(1):45–51

Yi Z, Jihong F, Shuilin C (2005) Dyeing of polyester using microencapsulated disperse dyes in the absence of auxiliaries. Color Technol 121(2):76–80. https://doi.org/10.1111/j.1478-4408.2005.tb00255.x

Yılmaz F (2020) Investigating the usage of eucalyptus leaves in antibacterial finishing of textiles against Gram-positive and Gram-negative bacteria. J Text Inst. https://doi.org/10.1080/00405000.2020.1753394

Zhao Q, Feng H, Wang L (2014) Dyeing properties and color fastness of cellulase-treated flax fabric with extractives from chestnut shell. J Clean Prod 80:197–203. https://doi.org/10.1016/j.jclepro.2014.05.069